16TH EUROPEAN CONFERENCE ON EARTHQUAKE ENGINEERING THESSALONIKI 18 - 21 JUNE 2018

DAMAGE EVALUATION OF RC BUILDING WITH SOIL-STRUCTURE INTERACTION BY SEISMIC INTERFEROMETRY: A NUMERICAL CASE STUDY

Fernando LOPEZ-CABALLERO[1], E. Diego MERCERAT[2]

ABSTRACT

A numerical study is presented representing a realistic soil-structure interaction (SSI) model under seismic loading. The studied case is composed of an 8-story reinforced concrete building founded over a layered soil. The aim of this work is to assess numerically the role of the non-linear soil behaviour on both the seismic response of structure and on its seismic damage assessment. Several 2D finite element models are carried out using a realistic non-linear elastoplastic model to represent both the soil behaviour and the building. Thus, several nonlinear dynamic analyses are performed in a parametric analysis. For this reason, appropriate input ground motions are chosen to enforce the inelastic behaviour of the soil. In order to track the evolution of induced structural damage, seismic interferometry by deconvolution of the numerical signals allows easy identification of normal modes of the SSI system and the structure alone (i.e. rigid base condition). Apparent wave velocities in the building estimated from the deconvolved signals (Impulse Response Functions IRF) are consistent with the input model parameters. Special focus on the different contributions of seismic attenuation and strategies to measure them from the IRF are discussed.

Keywords: Soil-structure interaction; Finite element method; Seismic interferometry

1. INTRODUCTION

Traditionally, in the earthquake engineering practice the soil-foundation-structure interaction phenomenon is studied with the assumption of the linear elastic behaviour for the soil. It is also well known that the seismic response of a structure can be significantly altered by the flexibility of its soil foundation. A numerical study is presented to study a realistic soil-structure interaction (SSI) under seismic loading. The studied case is composed of an 8-story reinforced concrete building founded over a layered soil. The aim of this work is to assess numerically the role of the non-linear soil behaviour on both the seismic response of structure and on its seismic damage assessment.
Several 2D finite element models are carried out using a realistic non-linear elastoplastic model to represent both the soil behaviour and the building. Thus, several nonlinear dynamic analyses are performed in a parametric analysis. For this reason, appropriate input ground motions are chosen to enforce the inelastic behaviour of the soil.
In this context, it is proposed to use seismic interferometry by deconvolution in order to assess SSI effects on the structure response. This approach considers the seismic response of the structure not as a vibration problem but as a wave propagation problem (Snieder and Safak, 2006). Seismic interferometry is a classical technique to estimate the Green's function between pair of receivers, and it has been widely used in the past years for many different studies of site characterization (Mehta et al, 2007, Parolai et al., 2010, Pilz et al., 2012; Hanneman et al., 2014), monitoring of oil and gas reservoirs (Bakulin and Calvert, 2006; Bakulin et al, 2007) and monitoring volcanoes and fault zones (Brenguier et al, 2008).

[1]Associate Professor, Laboratory MSSMat CNRS UMR 8579, CentraleSupélec, Paris-Saclay University, Gif-sur-Yvette, France, fernando.lopez-caballero@centralesupelec.fr
[2]Researcher, CEREMA Méditerrannée, MouvGS, Sophia-Antipolis, Nice, France, diego.mercerat@cerema.fr

Not long ago it started to be applied to buildings, enabling to observe the incident wave propagation across the structure, being nowadays the object of several studies using both earthquake and ambient vibrations recordings (Snieder and Safak, 2006; Kohler et al., 2007; Todorovska and Trifunac, 2008a; Prieto et al., 2010; Nakata and Snieder, 2014; Bindi et al., 2015; Michel and Gueguen, 2017). In such manner, interesting characteristics of the dynamic response of the building can be estimated, other than frequencies and damping.
Nakata et al. (2013) observed that wave velocities obtained from seismic interferometry in buildings are much more stable when using ambient noise vibrations than earthquake data. This is due to the fact that different input motion levels can affect the dynamic response of the structure, both in terms of changes in its elastic parameters and/or differences in the soil-structure interaction. In this paper, the effect of input motion levels on the results of seismic interferometry, through several realistic numerical simulations that take into account soil-structure interactions and non-linear soil behaviour is studied.

2. NUMERICAL MODEL

2.1 Geometry and Finite Element model

The studied building has 8 levels and a total height of 28m. The lateral-force-resisting system is constituted by moment resistant frames in longitudinal direction y (Figure 1a). The structure's Finite Element (FE) model is constructed with one-dimensional beam-column elements (Saez et al. 2011) using GEFDyn Code (Aubry et al. 1986). So as to study the effect of soil foundation on the structural response, a typical layered soil/rock model is considered. The soil profile is composed principally of medium dense sand. The total thickness of the soil profile is 30m over the bedrock. In the bottom, a layer of 5 m of elastic bedrock is added to the model. The shear wave velocity of the soil increases with depth. For the soil profile, a low-strain frequency analysis provides an elastic fundamental frequency near to 1.7Hz (Figure 2). It is obtained from the transfer function at free field (FF) condition (i.e. ratio of the frequency response at the soil surface over the bedrock frequency response for a sample seismic signal at very low amplitude to ensure elastic soil behaviour). An elastoplastic multi-mechanism model is used to represent the soil behaviour (Hujeux, 1985).
2D finite elements computations with a modified plane-strain approach (Saez et al., 2013) for the soil are performed. The soil is modelled using quadrilateral isoparametric elements with four nodes. A finer mesh is used in the neighborhood of the structure foundation to improve the approximation of non-linear behavior in this zone. The characteristic lengths of solid elements have been chosen small enough to prevent numerical dispersion problems. The thickness of the soil plane-strain elements is 4m. An implicit Newmark numerical integration scheme with $\alpha = 0.625$ and $\beta = 0.375$ is used in the dynamic analysis. The corresponding numerical damping ξ is approximately 0.1 %. It is important to remark that this numerical damping affects principally the elastic response of the model (i.e. $\gamma \leq 10-5$), and for greater values of γ the damping is provided by the material degradation (Montoya-Noguera and Lopez-Caballero, 2016).
In the SSI analysis, only vertically incident shear waves are introduced into the domain and the lateral limits of the problem are considered to be far enough from the structure, so that periodic conditions are verified on them as the response of an infinite semi-space is modelled. Equivalent boundaries have been imposed on the nodes of lateral boundaries (i.e. the normal stress on these boundaries remains constant and the displacements of nodes at the same depth in two opposite lateral boundaries are the same in all directions).
For the bedrock's boundary condition, paraxial elements simulating a "deformable unbounded elastic bedrock" have been used (Modaressi and Benzenati, 1994). The incident waves, defined at the outcropping bedrock are introduced into the base of the model after deconvolution. Thus, the obtained movement at the bedrock is composed of the incident waves and the reflected signal.

2.2 Soil constitutive model

The elastoplastic multi-mechanism model developed at *Ecole Centrale Paris*, known as ECP model (Hujeux, 1985) is used to represent the soil behaviour. This model can take into account the soil behaviour in a large range of deformations. The model is written in terms of effective stress. The

representation of all irreversible phenomena is made by four coupled elementary plastic mechanisms: three plane-strain deviatoric plastic deformation mechanisms in three orthogonal planes and an isotropic one. The model uses a Coulomb-type failure criterion and the critical state concept. The evolution of hardening is based on the plastic strain (deviatoric and volumetric strain for the deviatoric mechanisms and volumetric strain for the isotropic one). To take into account the cyclic behaviour a kinematical hardening based on the state variables at the last load reversal is used. The soil behaviour is decomposed into pseudo-elastic, hysteretic and mobilized domains. The detailed study of this model is beyond the scope of this work but refer to Aubry et al. (1986), Hujeux (1985), Lopez-Caballero and Modaressi-Farahmand-Razavi (2010) among others for further details about the ECP model. Figure 1b shows the responses of a cyclic shear test obtained by the ECP model for the set of parameter used between 2-30m depth, for three different initial confinement.

2.3 Structural model

The 8-story structure is shown in Figure 1. The total height of the building is 28m and the width is 26.5m. With these characteristics, the first fixed base frequency mode of the structure (f_{str}) is equal to 1Hz. The frame structural elements are modelled by plastic hinge beam-column elements. The model is based on the two-component model presented by Giberson (1969) and the modifications introduced by Prakash et al. (1993) to take into account axial force (P) and bending moment (M) interaction by specifying P-M yield surfaces. Refer to Prakash et al. (1993) and to Saez et al. (2011) for further details about the used model.

Before proceeding to the analysis, a computation of the soil–structure interaction phenomenon assuming elastic behaviour for both the soil and the structure is performed. Thus, transfer functions for the soil and the structure are computed, as well as the soil–structure interaction transfer function, given by the ratio of the frequency response on the top of the structure over the FF frequency response. Figure 2 shows the transfer function for the structure founded on fixed base as well as the one of the soil foundation at FF. It is noted that there is a small shift (less than 10%) in the fundamental frequency of the building to lower values, when the foundation is free to follow the ground movement, as well as to rotate. The largest frequency shift is found for the 3rd bending mode of the building (5 Hz) which is the closest to the 2nd resonant frequency of the soil (5.1 Hz). In addition, at the resonance frequency of soil–structure interaction the amplitude of the response of the structure is lower than the one at fixed base.

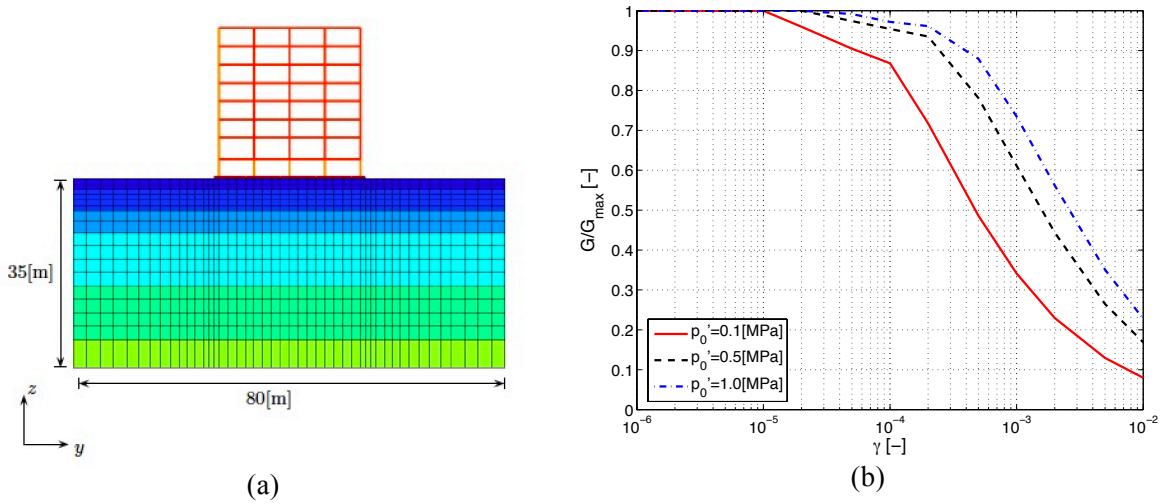

Figure 1. a) Used finite element model mesh (Saez et al. 2011) and b) Simulated drained cyclic shear test using ECP constitutive model (2 - 30m depth)

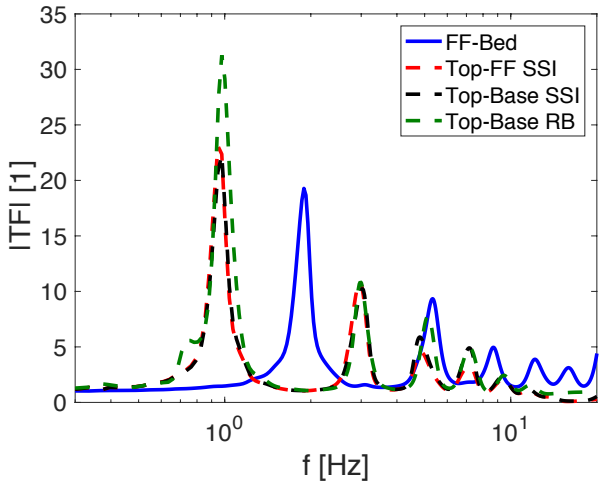

Figure 2. Obtained soil–structure interaction transfer functions assuming elastic behaviour for both soil and structure. FF (Soil free field), Top (Top of structure), Base (Base of structure), RB (Fixed base assumption) and SSI (Soil Structure interaction assumption).

2.4 Input earthquake motion

In order to define appropriate input motions to the non-linear dynamic analysis, a selection of 40 unscaled recorded accelerograms are used in outcropping bedrock condition. The used signals are from earthquakes related to subduction zone, which generates two types of events interface (shallow dipping thrust events) and intraslab (deep generally normal-faulting events). In addition, large crustal events were also selected. The adopted earthquake signals are proposed by Douglas (2006). Concerning the response spectra of input earthquake motions, Figure 3 shows the mean and the response spectra curves (structural damping ξ=5%) of the input motions.

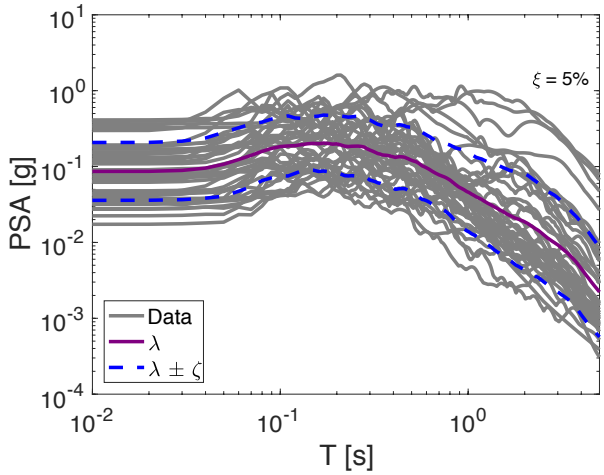

Figure 3. Response spectra of input earthquake motions (5% damped).

3. SEISMIC INTERFEROMETRY

In this study, the seismic interferometry is used to extract the building impulse response (IRF) by deconvolving the waves recorded at all floors with the waveform recorded at the top floor of the building. The deconvolution of two signals u(x) and u(x_{ref}) is done in the frequency domain by the expression:

$$D(x,\omega) = \frac{U(x,\omega)}{U(x_{ref},\omega)} \quad (1)$$

which may be unstable near the notches in the spectrum of $u(x_{ref})$. To stabilize the deconvolution, the following estimator for the deconvolution is used:

$$D(x,\omega) = \frac{U(x,\omega)\, U^*(x_{ref},\omega)}{U(x_{ref},\omega)^2 + e} \quad (2)$$

where the asterisk denotes the complex conjugation. In this work, the parameter *e* was set to 1 % of the maximum spectral power.

The deconvolved response gives the system impulse response function (IRF), which represents the system response to a virtual source at the location of the reference point (usually the roof) (Snieder and Safak, 2006). For a clearer interpretation, it is highlighted that the deconvolution by the bottom represents a spectral division by the input motion, enhancing the modal content of the structure, and hence creating stationary signals in the interferograms. On the other side, the deconvolution by the top represents a spectral division by the frequency content at the top of the building, dominated itself by its modal content, and hence removing the participation of the stationary modes. It leaves only an upgoing-downgoing wave that propagates through the building without making it enter in resonance.

The increase in the wave travel time *t*, detected by seismic interferometry, can be used as an indicator of possible damage. Analyses of recorded earthquake response in damaged buildings have shown that identified increases in *t* are consistent with the presence, distribution and severity of observed damage (Todorovska and Trifunac, 2008b, Rahmani and Todorovska, 2013). It is also possible to compare the relative amplitudes of upgoing and downgoing waves in order to estimate the attenuation through the medium.

4. NUMERICAL RESULTS

4.1 Soil response

In order to study the effect of the soil behaviour on the obtained acceleration at the base of the structure for the soil-structure case, Figure 4 shows the obtained values of the maximum ground acceleration (a_{max}) obtained at both free field and structure base with respect to maximum acceleration amplitude at outcropping bedrock ($a_{max\ out}$) for the selected earthquakes. It is noted that for lower acceleration values of the outcropping signal and due to the soil profile characteristics, an amplification of two times the acceleration imposed at outcropping is obtained at the surface level. It is also noted that due to soil non-linearity the amplification of the ground response decays with the amplitude of the input signal.

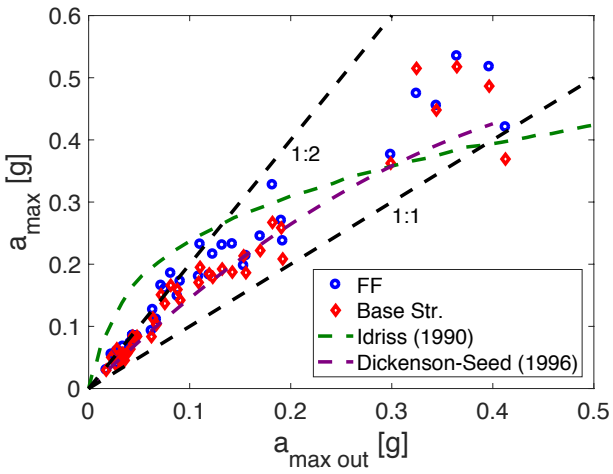

Figure 4. Scatter plot of maximum accelerations at outcropping bedrock and both obtained soil profile surface (FF) and structure base (Base Str.) for different input earthquakes.

4.2 Structural response

In order to study the effect of both the input signal and the presence of soil foundation on the building induced damage, multiple global parameters of seismic response could be used, interstory drift ratio (ISD), overall damage index (DI_{ov}), among others. ISD is a parameter that measures the relative horizontal displacement between the floor and ceiling of a story normalized by the inter-story height. According to the empirical observations and theoretical dynamic response studies, a strong correlation exists between magnitude of the ISD and the building damage potential. On the other hand, so as to take into account the damage due to inelastic behaviour in the building, as well as the damage due to the history of induced deformations an overall damage index could be used. In this work, and according to Saez et al. (2011), the used damage index is based on the damage model for reinforced concrete introduced by Park and Ang (1985). As the inelastic behaviour is confined to plastic zones near the ends of some members, the relation between element and overall structure integrity is not direct. According to the used structural non-linear model, for each potential hinge *i*, it is possible to compute a local index of damage ($DI_{loc,i}$). This local index is a function of the maximum rotation reached during the load history in the plastic component, the ultimate rotation capacity and the yield moment of the plastic component. Following Hwang and Huo (1994) and Saez et al. (2011), the overall damage index is computed using weighting factors based on dissipated hysteretic energy at each potential hinge *i* :

$$DI_{ov} = \sum_i \lambda_i \, DI_{loc\,i} \tag{3}$$

where λ_i is the energy weighting factor of the potential hinge *i*. This parameter was calibrated in terms of ultimate plastic hinge rotations observed during incremental pushover test. Refer to Saez et al. (2011) for more details about this parameter. Figure 5 displays the computed overall damage index of the building as a function of the maximum value of the computed inter-story drift (ISD_{max}) for all the records when a rigid base condition is assumed. It is observed that a good agreement between this two parameters is obtained and also that the total collapse is found (i.e. a DI_{ov} equal to 1) for some cases. In the follows, only the overall damage index will be used to describe the potential damage of the building.

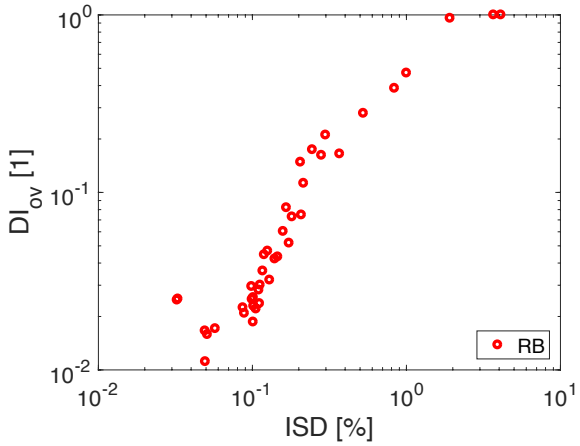

Figure 5. Scatter plot of obtained overall damage index as a function of normalized maximum inter-story drift.

Figure 6a displays the DI_{ov} value obtained for each record as a function of the of pseudo-spectral acceleration (PSA) at the fundamental structural period (T=1s) at outcropping bedrock for the case with and without SSI. It is observed that for both cases, the higher the pseudo-spectral acceleration level, the higher the induced damage. To account for the effect of the presence of soil foundation on the response of the induced building damage a scatter plot comparing the obtained DI_{ov} values for the rigid base condition ($DI_{ov\,RB}$) with the ones obtained in SSI condition ($DI_{ov\,SSI}$) for the same outcropping motion is shown in Figure 6b. It is interesting to note that, as expected for this particular case (Figure 4), for the majority of cases the induced damage increases if the SSI is taken into account.

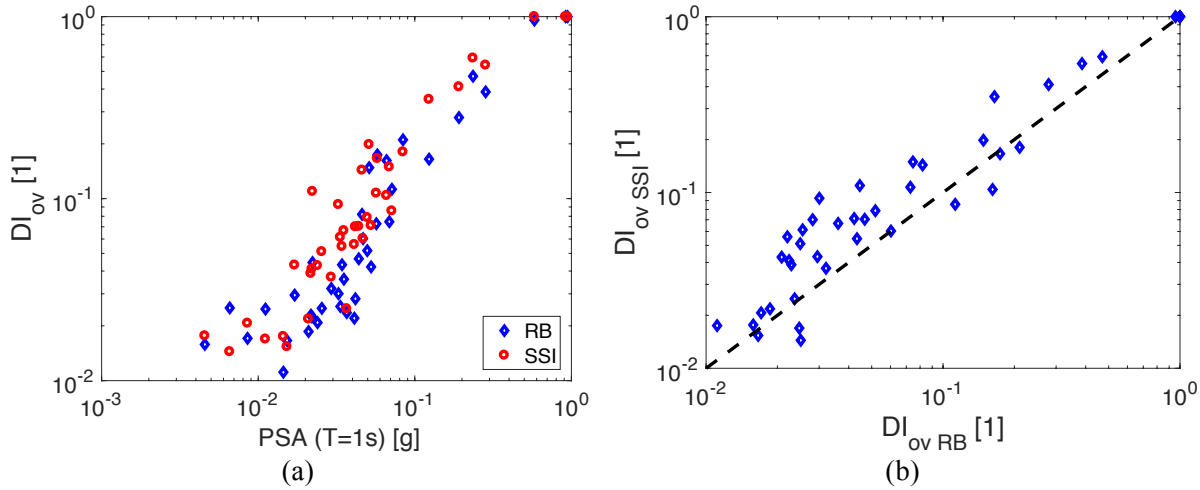

Figure 6. a) Computed overall damage index as a function of pseudo-spectral acceleration (PSA) at the fundamental structural period at outcropping bedrock for rigid base condition and SSI; and b) Comparison of the overall damage index obtained for rigid base condition and SSI condition.

Figure 7 displays the nonlinearity evolution of the soil structure system by analyzing the transfer function (TF) between the top of the building and the free field (FF). This function takes into account the structure's performance as well as the SSI effects. Three cases with three different DI_{ov} values are shown, 0.02, 0.41 and 0.54. It is observed a lower amplitude of the two first predominant frequencies when the DI_{ov} value increase from 0.02 (close to elastic behaviour) to 0.41. This deamplification increases drastically when the DI_{ov} value is equal to 0.54.

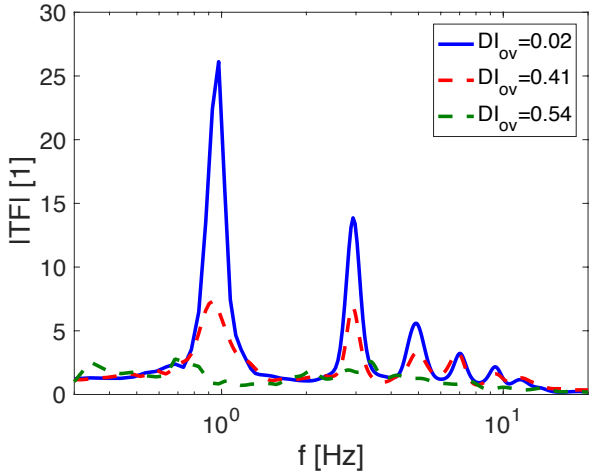

Figure 7. Nonlinearity evolution at the structure's |TF| (Top/FF) with the overall damage index.

4.3 Interferometry results

Seismic interferometry by deconvolution using equation (2) represents the system response to a virtual source placed at the roof of the building as reference. A bandpass filter is applied to all signals before deconvolution in the frequency band of interest here (0.1-10 Hz). In such way, the deconvolved signals are composed of an upgoing wave entering the structure from the bottom, traveling upwards through the structure, reflected from the free surface at the top, and traveling downwards to the bottom sensor. The travel time is close to 0.243s for both waves which gives an apparent seismic velocity close to 115m/s. This apparent velocity corresponds to a building presenting pure shear behaviour with a frequency of the first bending mode (f_0) equal to $V^*/4H = 1.04$Hz.

After carefully analysis of the interferograms, upgoing and downgoing apparent wave velocities are

determined by picking of the maximum of the waveforms both in the acausal (upgoing) and causal (downgoing) parts (Figure 8). Apparent velocities from upgoing/dowgoing waves are not significantly different, unless for small values of input PGAs. It should be stressed that this picking is not straightforward, specially in the case of relatively large input motion levels, as the waveforms may be completely distorted when traveling through the building. In fact, as it can be seen from Figure 9, the picked wave velocities are no longer reliable for interferograms corresponding to high DI_{ov} values (> 0.1). In contrast, the ratio of downgoing/upgoing amplitudes at the same level of the building (in this case at the ground floor) is well correlated with the damage index independently of DI_{ov} value (Figure 10). Then this parameter appears to carry important information in terms of structural damage assessment.

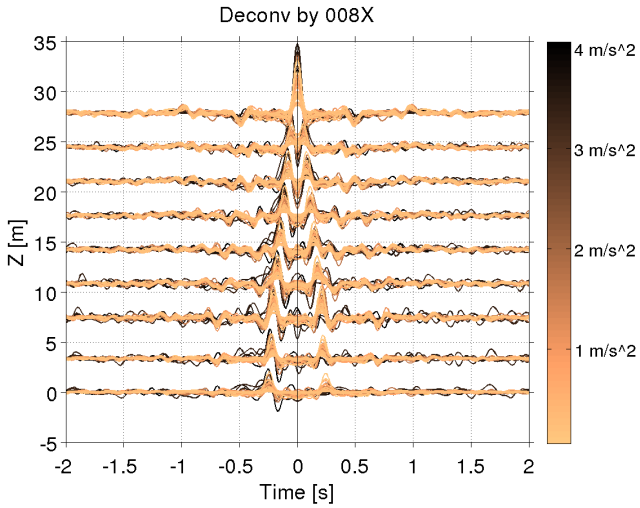

Figure 8. Seismic interferograms (deconvolution by the sensor at the top) at different heights of the building (Z=0m ground floor, Z=28m top floor). Color scale for different input levels of PGA.

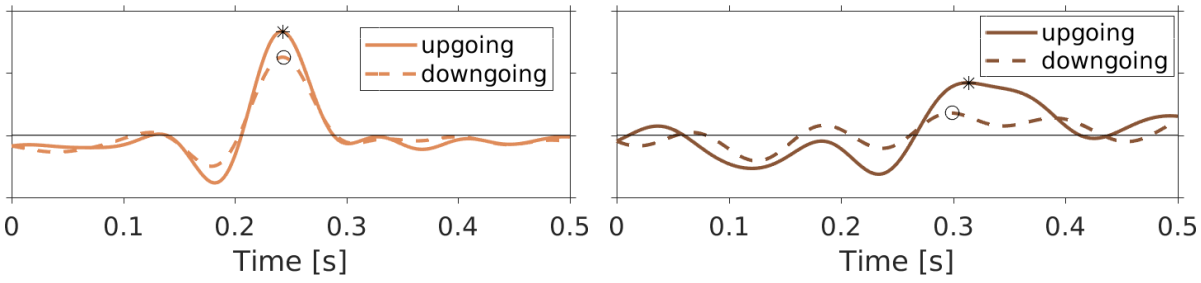

Figure 9. Selected interferograms (deconvolution by the sensor at the top) at Z=0m for two different input motions: (left) DIov=0.04, and (right) DIov=0.54. The picks corresponding to the maximum amplitudes are also shown for the upgoing (reversed time axis) and downgoing waves.

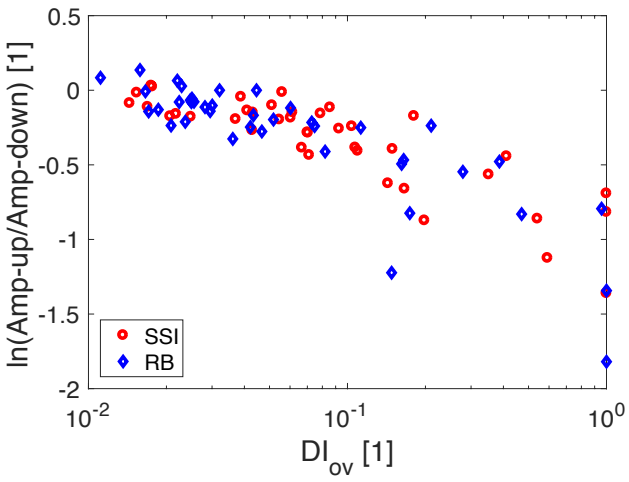

Figure 10. Relative amplitudes at the sensor at the bottom from the acausal (upgoing) and causal (downgoing) waveforms

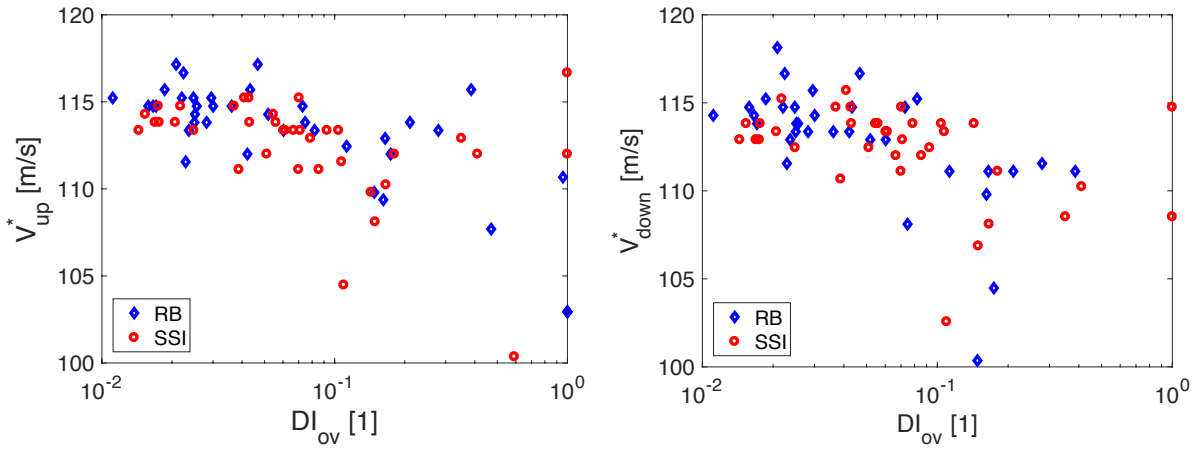

Figure 11. Seismic velocities in function of damage index inferred from interferometry picks at Z=0m (left) from upgoing (left) and downgoing (right) waveforms

Lastly, it is noted in Figure 11 a slight decrease (< 5%) in the apparent velocity through the building as function of damage index. It seems to be true for low DIov values (< 0.1) although the relatively large dispersion. For higher values, the picked velocities are no longer meaningful and the correlation is lost. It should be noted that in this case, when the structure is considerably damaged due to the seismic excitation, the hypothesis of a linear medium for seismic interferometry by deconvolution may no longer be valid.

5. CONCLUSIONS

The soil-structure interaction of a high-rise building over a deformable soil was studied numerically. Several recorded signals were used so as to induce a large range of damage level into the building. The use of seismic interferometry by deconvolution allowed to identify parameters that could be used in real cases so as to control the damage level of the structure. The modeled building presents a classical shear behaviour as established by the ratio between measured frequencies.

Frequency shift to lower frequencies are more pronounced for normal modes closer to the resonant peak of the soil (3rd one in our case study).

Apparent wave velocities in the building estimated from the deconvolved signals are consistent with the input model parameters and the hypothesis of shear behaviour of the building. These apparent velocities appear to be less sensitive to induced damage level than relative amplitudes from upgoing-downgoing waveforms. This may be caused by the fact that just one upgoing-downgoing path in the structure is analyzed. It is possible that using deconvolution by the bottom (use of stationary waves in the structure)

allows to more reliably pick apparent velocities in the structure. However, the fact that the structure is damaged during the seismic excitation may be at odds with the hypothesis of stationarity of the medium use in seismic interferometry. The monitoring of seismic velocities can be used as proxy for damage evolution only in the case of comparing stationary signals (i.e. ambient vibrations) during interseismic periods. Measurement of relative amplitudes between upgoing/downgoing waves (as a proxy for attenuation in the structure) is highly correlated with damage index independently of soil-structure or rigid-base boundary conditions.
Further works concern the track of the temporal changes of both the local and global properties of the building using divers techniques as for example the short time Fourier Transform spectral ratio.

6. ACKNOWLEDGMENTS

This work has been done in the framework of AO RAP 2017 French project: *Caractérisation de l'ISS à partir de données accélérométriques et de mesures de vibrations ambiante*s and it was also partly supported by the SEISM Paris Saclay Research Institute. These supports are gratefully acknowledged.

7. REFERENCES

Aubry, D., Chouvet, D., Modaressi, A., Modaressi, H. (1986). "GEFDYN: Logiciel d'analyse de comportement mécanique des sols par eléments finis avec prise en compte du couplage sol-eau-air". Manuel scientifique, Ecole Centrale Paris, LMSS-Mat.

Bakulin, A., Calvert, R., 2006. The virtual source method: Theory and case study. *Geophysics*.71(4), SI139-SI150.

Bindi D, Petrovic B, Karapetrou S, Manakou M, Boxberger T, Raptakis D, Pitilakis KD, Parolai S (2015) Seismic response of an 8-story RC-building from ambient vibration analysis. *Bulletin of Earthquake Engineering*, 13(7): 2095-2120.

Brenguier, F., Campillo, M., Hadziioannou, C., Shapiro, N. M., Nadeau, R.M., Larose, E. (2008). Postseismic relaxation along the San Andreas fault at Parkfield from continuous seismological observations. *Science*. 321(5895), 1478-1481.

Dickenson, S. and Seed, R. (1996). Nonlinear dynamic response of soft and deep cohesive soil deposits. In Proc. of the International Workshop on Site Response Subjected to Strong Earthquake Motions. Yokosuka, Japan.

Douglas, J. (2006). Selection of strong-motion records for use as input to the structural models of veda. Report BRGM BRGM/RP-54584-FR, BRGM.

M. Giberson, M. (1969). Two non-linear beams with definitions of ductility. *J Struct Div ASCE*, 95(2):137-157.

Hannemann, K., Papazachos, C., Ohrnberger, M., Savvaidis, A., Anthymidis, M., Lontsi, A.M., (2014). Three-dimensional shallow structure from high-frequency ambient noise tomography: New results for the Mygdonia basin-Euroseistest area, northern Greece. *Journal of Geophysical Research: Solid Earth*.119(6), 4979-4999.

Hujeux, J.-C. (1985). " Une loi de comportement pour le chargement cyclique des sols. In Génie Parasismique". V. Davidovici, Presses ENPC, France., 278–302.

Hwang, H., Huo, J.-R. (1994). Generation of hazard-consistent fragility curves. *Soil Dynamics and Earthqauke Engineering*, 13(5):34–354.

Kohler MD, Heaton TH, Bradford SC (2007) Propagating waves in the steel, moment-frame factor building recorded during earthquakes. *Bulletin of the Seismological Society of America*, 97(4):1334-1345.

Lopez-Caballero, F., Modaressi-Farahmand-Razavi, A. (2010). Assessment of variability and uncertainties effects on the seismic response of a liquefiable soil profile. *Soil Dynamics and Earthquake Engineering*, 30(7):600–613.

Mehta, K., Snieder, R., Graizer, V., (2007). Downhole receiver function: a case study. *Bulletin of the Seismological Society of America*. 97(5):1396-1403.

Michel C and Gueguen Ph, (2018). Interpretation of the velocity measured in buildings by seismic interferometry based on Timoshenko beam theory under weak and moderate motion. *Soil Dynamics and Earthquake Engineering*. 104(1):131-142.

Modaressi, H., Benzenati, I. (1994). Paraxial approximation for poroelastic media. *Soil Dynamics and Earthquake Engineering*, 13(2), 117–129.

Montoya-Noguera, S., Lopez-Caballero, F. (2016). Effect of coupling excess pore pressure and deformation on nonlinear seismic soil response. *Acta Geotechnica*, 11(1):191–207.

Nakata, N., R. Snieder, S. Kuroda, S. Ito, T. Aizawa, and T. Kunimi, (2013) Monitoring a building using deconvolution interferometry. I: Earthquake-data analysis, *Bulletin of the Seismological Society of America*, 103, 1662-1678.

Nakata, N. and R. Snieder, (2014) Monitoring a building using deconvolution interferometry. II: Ambient-vibration analysis, *Bulletin of the Seismological Society of America*, 104, 204-213.

Park, Y., Ang, A. (1985). Mechanistic seismic damage model for reinforced concrete. *Journal of Structural Engineering, ASCE*, 111(4):722–739.

Parolai, S., Bindi, D., Ansal, A., Kurtulus, A., Strollo, A., Zschau, J., (2010). Determination of shallow S-waveattenuation by down-holewaveformdeconvolution: A case study in Istanbul (Turkey). *Geophysical Journal International*. 181(2), 1147-1158.

Prakash V, Powel G, Campbell S. DRAIN 2D-X: base program description and user guide. Dept. of Civil Engineering, University of California, Berkeley; 1993.

Pilz, M., Parolai, S., Picozzi, M., Bindi, D., (2012). Three-dimensional shear wave velocity imaging by ambient seismic noise tomography. *Geophysical Journal International*. 189(1), 501-512.

Prieto GA, Lawrence JF, Chung AI, Kohler MD (2010) Impulse Response of Civil Structures from Ambient Noise Analysis. *Bulletin of the Seismological Society of America* 100(5A):2322-2328.

Rahmani M, Todorovska MI (2013) 1D system identification of buildings during earthquakes by seismic interferometry with waveform inversion of impulse responses-method and application to Millikan library. *Soil Dynamics and Earthquake Engineering*, 47(1): 157-174.

Saez, E., Lopez-Caballero, F., Modaressi-Farahmand-Razavi, A. (2011). Effect of the inelastic dynamic soil-structure interaction on the seismic vulnerability assessment. *Structural Safety*, 33(1):51–63.

Saez, E., Lopez-Caballero, F., Modaressi-Farahmand-Razavi, A. (2013). Inelastic dynamic soil-structure interaction effects on moment-resisting frame buildings. *Engineering Structures*, 51(1):166–177.

Snieder R, Safak E. (2006) Extracting the building response using interferometry: theory and applications to the Millikan Library in Pasadena, California. *Bulletin of the Seismological Society of America*, 96(2):586–98.

Todorovska MI, Trifunac MD (2008a) Impulse response analysis of the Van Nuys 7-storey hotel during 11 earthquakes and earthquake damage detection. *Structural control and health monitoring* 15(1):90-116

Todorovska MI, Trifunac MD. (2008b) Earthquake damage detection in the Imperial County Services Building III: analysis of wave travel times via impulse response functions. *Soil Dynamics and Earthquake Engineering*, 28(5):387–404.